

CALCULATION OF THE MIXED NEUTRON-GAMMA REFERENCE FIELDS CHARACTERISTICS

Kluson, J.

Faculty of Nuclear Sciences and Physical Engineering, CTU Prague
Břehová 7, 115 19 Prague 1, Czech Republic
kluson@fjfi.cvut.cz

Jánský, B.

Nuclear Research Institute, Řež
Husinec - Řež, 130, 250 68 Řež, Czech Republic
jan@ujv.cz

ABSTRACT

Set of the spherical experimental assemblies for the mixed neutron-gamma reference fields implementation was build in the Experimental Reactor Physics Department in NRI Rez. Extended studies of the mixed fields characteristics/parameters including Monte Carlo mixed fields simulations, neutron and gamma flux and spectra experimental measurements and benchmark tests were done. Different experimental setups models and simplifications were tested and results of the calculations compared. Some “secondary” effects (mostly hard to estimate experimentally) were studied: the shielding cones transparency and contribution of the secondary particles from interaction in the cone for both (neutron and gamma) components, contributions of individual components (direct radiation, scattering in the air/floor, interactions/scattering in the cone), influence of the real source arrangement (transport box, pneumatic rabbit holder, transport channel plugging) on the mixed field dependence on the elevation (polar) angle. Interference of the assemblies in the experimental hall was assessed. Results for basic configurations were compared with experimental data. Results of the mentioned above calculations are presented and discussed.

Key Words: mixed neutron-gamma reference fields, Monte-Carlo method, radiation transport simulation, neutron and gamma spectra, shadow shield technique

1 INTRODUCTION

Set of the spherical experimental assemblies for the mixed neutron-gamma reference fields implementation was build in the Experimental Reactor Physics Department in NRI Rez [1] with main aim to extend experimental base for reactor studies. The iron and water spherical assemblies with diameters 20, 30, 50, 100 cm and 30, 50 cm are available as well as set of the ^{252}Cf neutron sources with different emissions (positioned to the sphere center by pneumatic transportation system). Extended sets of measurements and simulation calculations were done to describe the reference mixed fields dosimetry and spectral characteristics with best achievable precision [2, 3].

1.1 Experimental Arrangement

The basic dosimetric characteristic – the neutron/photon flux density in the field reference point – are measured (as well as corresponding spectral distributions) by shadow shield

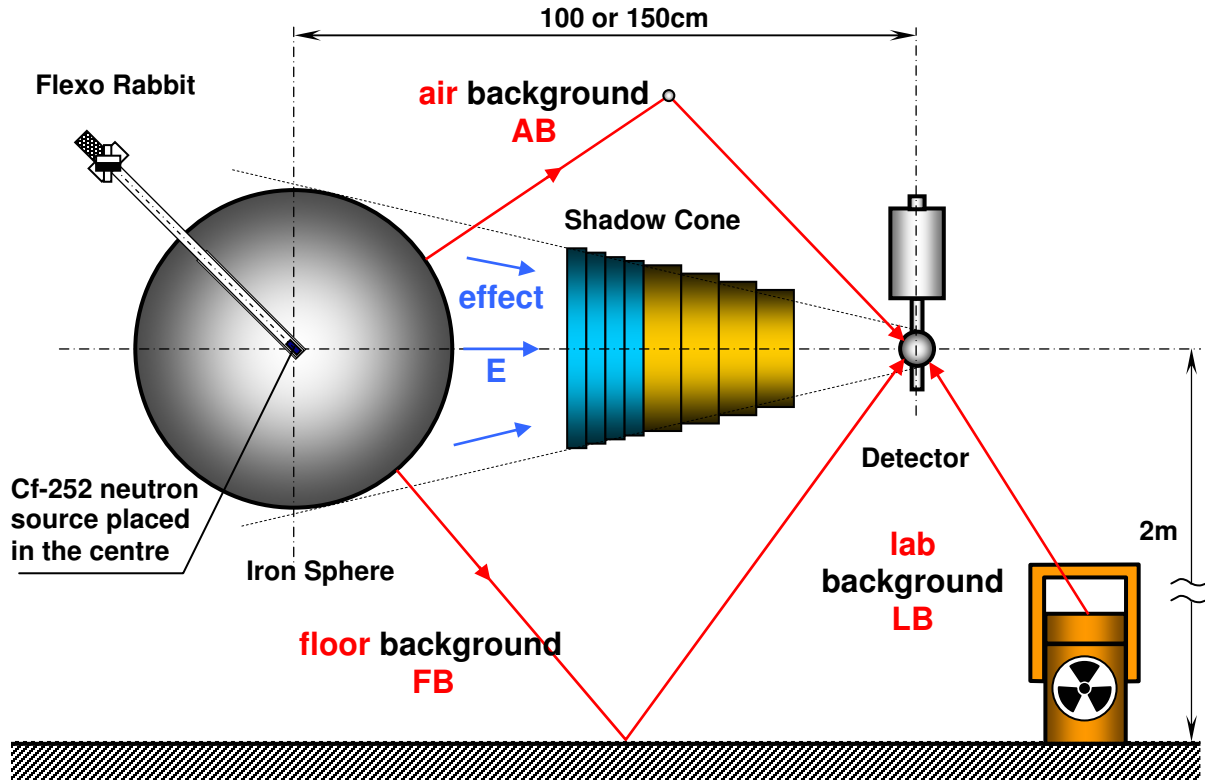


Figure 1: Schematic drawing of the experimental arrangement and field components.

technique. Measurements are performed typically at distance $R = 100$ cm (distance from the detector centre to the ^{252}Cf source centre) for spheres of diameter 20, 30, 50 cm and in distance $R = 150$ cm for iron sphere of diameter 100 cm. Individual assemblies are identified by abbreviated labels (used in the next text): Fe50R100 – arrangement with iron sphere of diameter 50 cm and reference point distance 100 cm, Fe100R150 – iron sphere with diameter 100 cm, distance 150 cm, etc. The additional measurements have been done on the distance 3 or 7 cm from sphere surface (the surface spectra). The spheres and detectors are positioned 2 meters above floor of experimental hall. The background component of the measured field is determined by measurement performed with shielding cones. Cones are designed and positioned to shield direct component in the corresponding space angle. The cone used for neutron shielding was made of 20 cm iron layer (source side) and 30 cm polyethylene with boron (3% weight) layer (detector side). The cone for gamma shielding consist of lead with thickness 21 cm. Schematic drawing of the experimental arrangement and field components is in the Fig. 1.

1.2 Methodology of Measurement

Net values of the measured quantities are determined by well known method when net effect (E) is determined as difference between the sum of net effect (E) and all background components (AB+FB+LB) measured in arrangement without shielding cone and sum of background components (AB+FB+LB) measured in arrangement with shielding cone removing measured effect contribution. In fact, some next secondary effects affect field in arrangements with shielding cones. Cone presence generally affects the primary field including measured background components. Measured values can be influenced by cone nonzero transparency for

radiation field components, by scattering in the cone, secondary photons emission due to neutron interactions in the cone, etc. Effect of these processes can't be differentiated and evaluated from experimental measurements. Therefore the transport simulation model was used for assessment of such processes.

2 CALCULATION OF THE MIXED FIELD COMPONENTS FOR THE FE50R100 EXPERIMENTAL ASSEMBLY

The models of experimental arrangements for both types of shielding cones (for neutrons and photons) were described for simulation using MCNPX code. Free space version and arrangement with floor of experimental hall were prepared. Arrangement with Pb cone (for photon shielding) is in Fig. 3 (view with floor), set-up with Fe+PE(B) cone (for neutron shielding) shows Fig. 2. The spherical approximation of the source and significant parts source

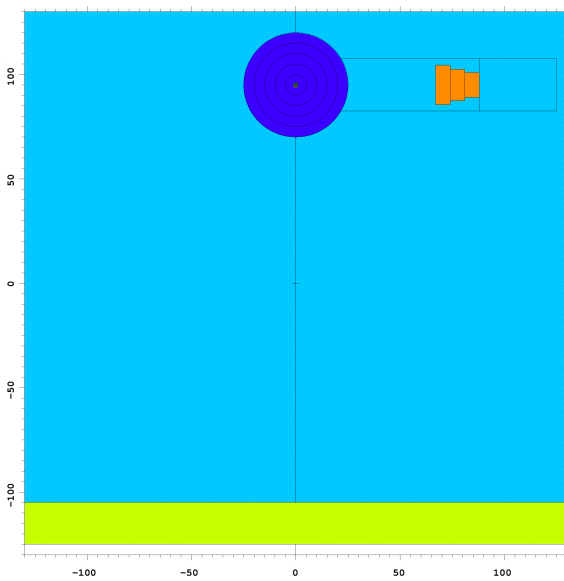


Figure 3: Arrangement with Pb shielding cone

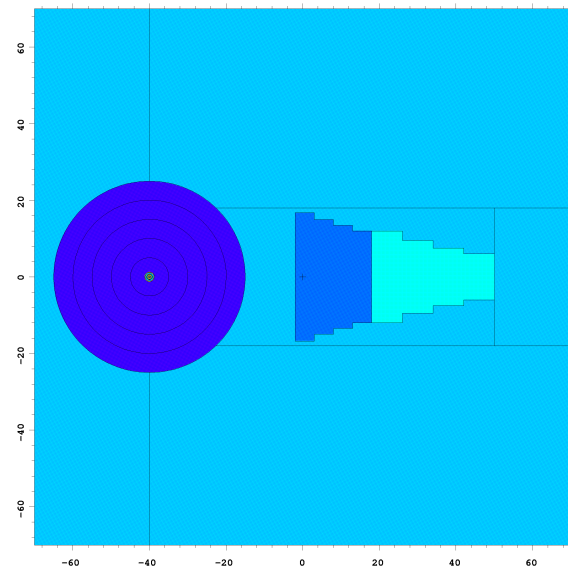


Figure 2: Arrangement with Fe+PE(B) shielding cone

transportation system was used. Set of calculations for the gamma/neutron source components, free space and “with floor” (20 cm concrete layer) arrangements and set-ups without shielding cone and with Pb or Fe+PE(B) cone were done (12 configurations). Contributions of the individual parts (source + sphere, air/floor/cone scattering) of set-up were calculated including spectral distributions (for the point detector in the reference position).

2.1 Results of Calculations

Results of calculations are shown in Table I (free space) and Table II (arrangement with floor). Contribution from source/sphere represents the net effect (without cone) or cones transparency (in arrangements with cones). Other items represent contributions of scattered/secondary radiation (sorted by last scattering/interaction event) originated from the air, floor and parts of shielding cone. Relative significance of individual contributions is illustrated by graphical presentation of these results in the bar graphs in Fig. 4 (comparison of photons total) and Fig. 5 (comparison for neutrons).

Table I : Results for the free space arrangement

Arrangement/ quantity Contribution	Free space							
	primary photons		secondary photons		photons (total)		neutrons	
	$4\pi R^2 \varphi(E)/Q$ [1]	error [%]	$4\pi R^2 \varphi(E)/Q$ [1]	error [%]	$4\pi R^2 \varphi(E)/Q$ [1]	error [%]	$4\pi R^2 \varphi(E)/Q$ [1]	error [%]
Without cone								
source/sphere	5.669E-03	0.20	3.324E-02	0.13	3.891E-02	0.14	9.687E-01	0.01
last scattering in air	8.473E-05	1.91	5.516E-04	1.05	6.363E-04	1.16	2.848E-02	0.25
last scattering in floor	-	-	-	-	-	-	-	-
total	5.754E-03	0.20	3.380E-02	0.13	3.955E-02	0.14	9.972E-01	0.01
With Pb cone								
source/sphere	5.407E-08	0.37	1.383E-07	0.20	1.924E-07	0.25	1.580E-02	0.01
last scattering in air	5.491E-05	1.33	3.558E-04	0.61	4.107E-04	0.71	2.181E-02	0.08
last scattering in cone	5.883E-07	40.52	6.666E-05	16.79	6.725E-05	17.00	1.815E-02	0.20
last scattering in floor	-	-	-	-	-	-	-	-
total	5.555E-05	1.40	4.226E-04	2.70	4.781E-04	2.55	5.576E-02	0.07
With Fe, PE+B cone								
source/sphere	1.226E-06	0.48	7.443E-06	0.36	8.669E-06	0.38	9.167E-08	0.85
last scattering in air	4.238E-05	1.11	3.707E-04	0.48	4.131E-04	0.54	1.663E-02	0.07
Fe cone (disc 1 - 4)	2.953E-06	2.26	3.543E-04	0.34	3.573E-04	0.36	5.726E-07	1.93
PE+B cone (disc 5 - 8)	4.184E-06	25.77	2.511E-03	0.52	2.515E-03	0.56	8.326E-04	2.45
last scattering in cone	7.137E-06	15.15	2.866E-03	0.46	2.873E-03	0.50	8.331E-04	2.45
last scattering in floor	-	-	-	-	-	-	-	-
total	5.074E-05	2.36	3.244E-03	0.41	3.294E-03	0.44	1.747E-02	0.13

Table II : Results for the arrangement with floor of the experimental hall

Arrangement/ quantity Contribution	With floor							
	primary photons		secondary photons		photons (total)		neutrons	
	$4\pi R^2 \varphi(E)/Q$ [1]	error [%]	$4\pi R^2 \varphi(E)/Q$ [1]	error [%]	$4\pi R^2 \varphi(E)/Q$ [1]	error [%]	$4\pi R^2 \varphi(E)/Q$ [1]	error [%]
Without cone								
source/sphere	5.675E-03	0.21	3.342E-02	0.16	3.9099E-02	0.17	9.698E-01	0.01
last scattering in air	9.983E-05	7.81	6.909E-04	0.85	7.9076E-04	1.73	3.334E-02	0.19
last scattering in floor	1.602E-04	0.20	3.931E-03	0.09	4.0910E-03	0.09	6.427E-02	0.02
total	5.935E-03	0.24	3.805E-02	0.14	4.3981E-02	0.15	1.067E+00	0.01
With Pb cone								
source/sphere	5.492E-08	1.62	1.393E-07	0.37	1.943E-07	0.72	1.580E-02	0.01
last scattering in air	6.124E-05	0.73	4.836E-04	0.60	5.448E-04	0.61	2.656E-02	0.08
last scattering in cone	1.071E-06	23.17	7.967E-05	3.48	8.074E-05	3.74	2.068E-02	0.21
last scattering in floor	1.597E-04	0.22	3.949E-03	0.09	4.109E-03	0.10	6.456E-02	0.02
total	2.220E-04	0.28	4.513E-03	0.12	4.735E-03	0.13	1.276E-01	0.04
With Fe, PE+B cone								
source/sphere	1.237E-06	1.32	7.522E-06	0.18	8.760E-06	0.34	9.242E-08	1.83
last scattering in air	4.732E-05	0.79	5.475E-04	4.85	5.948E-04	4.53	2.135E-02	0.09
Fe cone (disc 1 - 4)	3.110E-06	2.34	3.837E-04	0.35	3.868E-04	0.37	5.638E-07	1.90
PE+B cone (disc 5 - 8)	9.002E-06	9.95	4.627E-03	0.42	4.636E-03	0.44	3.285E-03	1.29
last scattering in cone	1.211E-05	7.43	5.011E-03	0.39	5.023E-03	0.41	3.285E-03	1.29
last scattering in floor	1.342E-04	0.23	4.109E-03	0.09	4.243E-03	0.09	6.626E-02	0.02
total	1.948E-04	0.53	9.675E-03	0.34	9.870E-03	0.34	9.089E-02	0.05

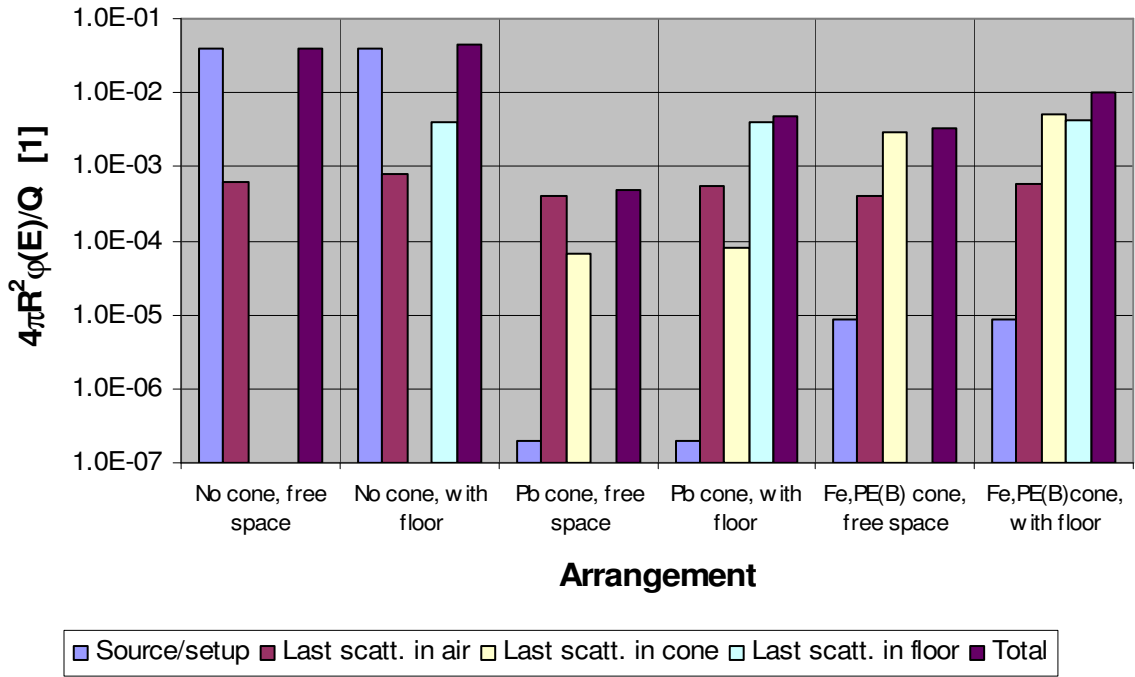


Figure 4: Total photon contributions

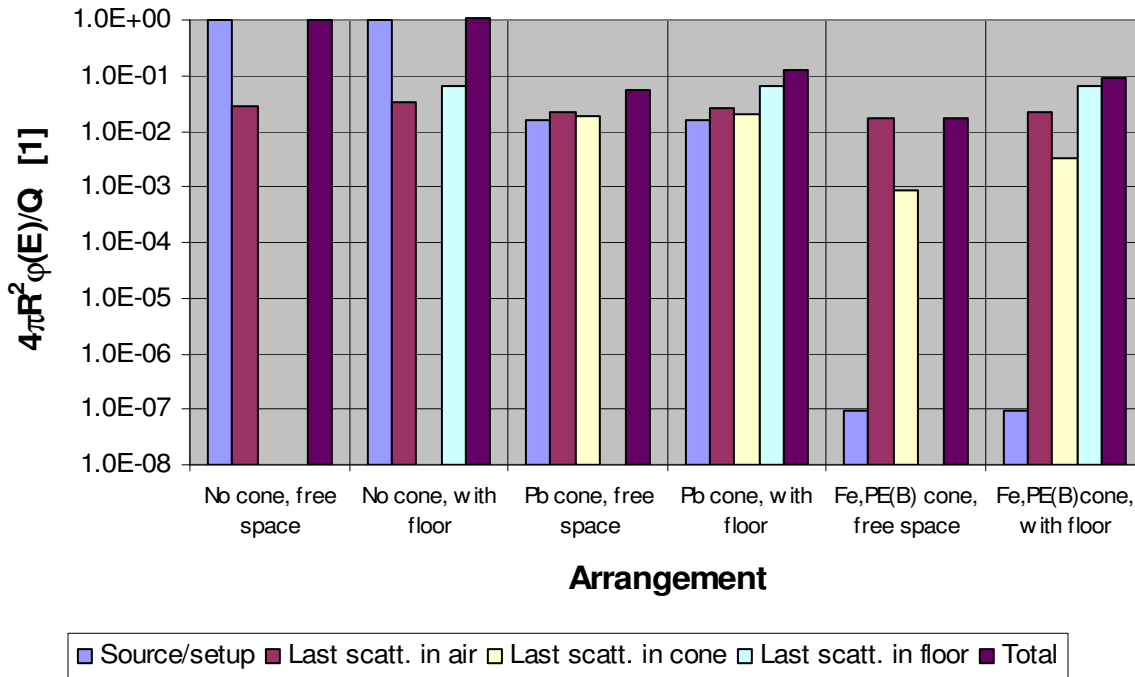


Figure 5: Neutron contributions

All results are normalized to source of unity neutron emission and multiplied by factor $4\pi R^2$ (expressed as dimensionless values). Examples of calculated spectral distributions of the photons and neutrons passed through or scattered/originated from Fe+PE(B) cone are in Figs. 6, 7. The

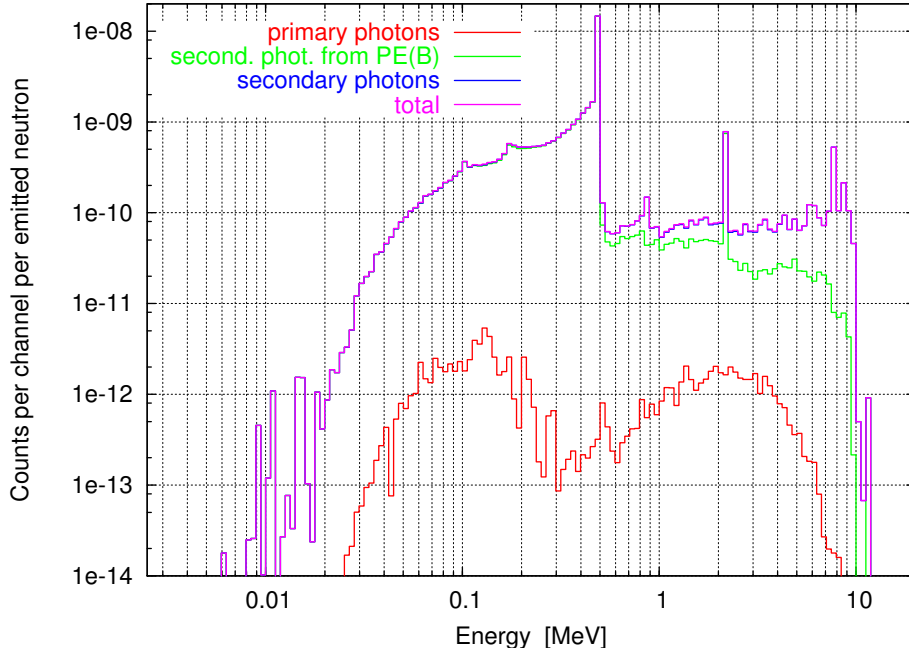


Figure 6 : FE50R100 set-up with floor, Fe+PE(B) cone, spectrum of total gamma through/from cone

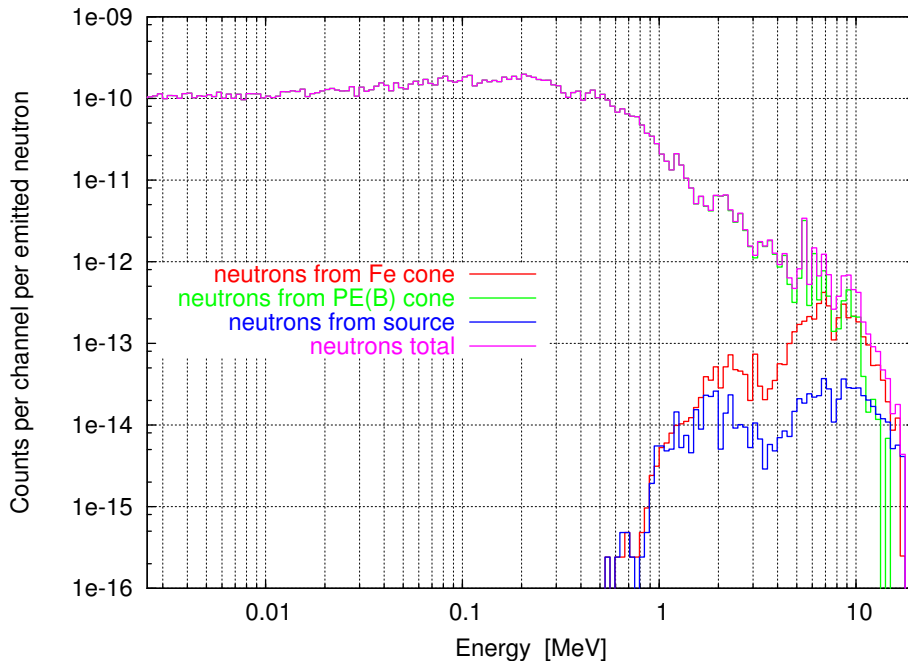


Figure 7 : FE50R100 set-up with floor, Fe+PE(B) cone, spectrum of neutrons through/from cone

typical peak (2.223 MeV) of secondary photons from interactions of neutrons with polyethylene (PE) part of cone is for example apparent in Fig. 6.

3 MIXED FIELDS HOMOGENEITY STUDIES

In the real experimental arrangement the set-up symmetry is violated by the source pneumatic transport channel, presence of rabbit holder, source transport box and unsymmetrical source shape. Influence of these asymmetries on the neutron-gamma fields were studied using Monte Carlo MCNP model with more detailed source and rabbit holder description. Influence and importance of the inner tube of rabbit holder plugging was also studied.

3.1 Model Description

Model of the FE50R100 experimental set-up with source transportation system (transport box and rabbit holder) full description was prepared. Versions for free space arrangement and with floor of the experimental were taken into account as well as versions with opened source transportation channel and arrangement when inner tube of the rabbit holder is plugged with iron rod (see Fig. 9). Detail of the rabbit holder head with no plug and with source in transport box

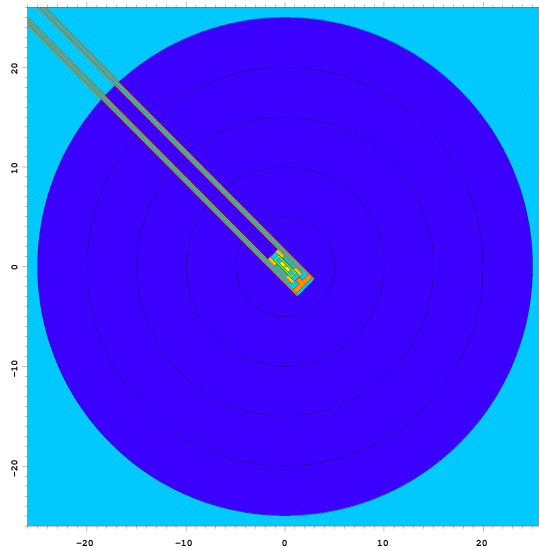


Figure 9: Arrangement with source and source transportation system full description

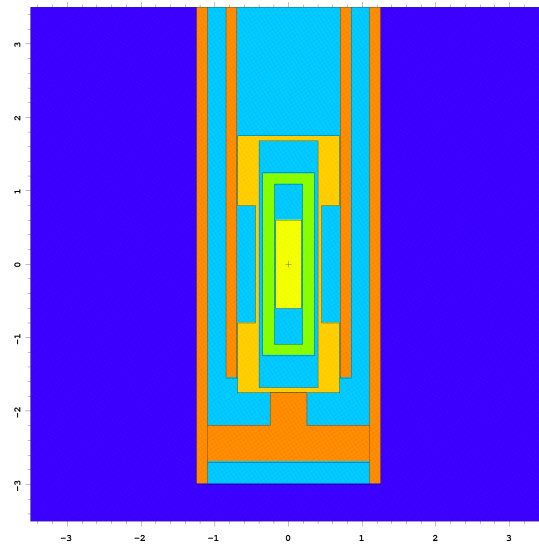


Figure 8: Detail of model description of the rabbit holder head with source in the transport box

model is in Fig. 8. Calculations were done for all model versions (see above) and for set of elevation (i.e. polar) angles of point detectors positions. Elevation angles were selected in the range from -45 deg up to 135 deg (angle 0 deg represents the reference point, angle 135 deg corresponds to the detector position on the transportation channel axis).

For comparison with simplified models the calculations were done also for the arrangement with the symmetrical approximation of the source and significant parts of transportation system and without transportation channel (see also Figs. 2, 3).

3.2 Results of Calculations

Calculated dependencies of the photon and neutron flux densities (normalized to the dimensionless values – see above) on the elevation angle are presented on the Fig. 10 (for photons) and Fig. 11 (for neutrons). Results for the simplified geometry are also included.

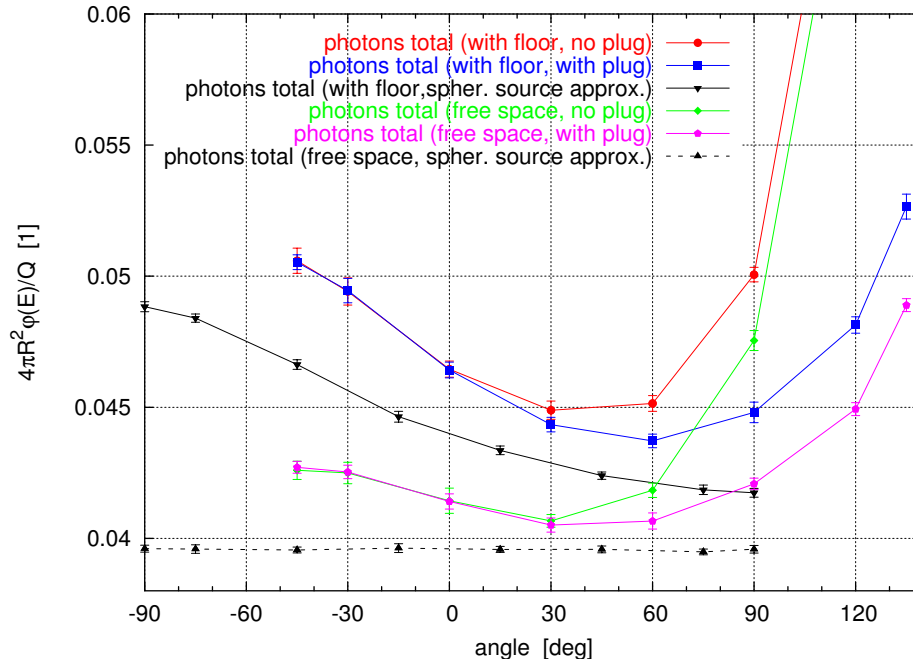


Figure 10: FE50R100 set-up, calculated dependence of the normalized photon flux density on angle of elevation (in the plane of rabbit holder, real detector position=0 deg, rabbit holder axis=135 deg, $\pm 2\sigma$ error bars)

Expected contribution from scattering in the floor (increasing for lower elevation angles) can be observed for photons as well as for neutrons. For upper elevation angles and models with full geometry description the increasing contributions of photons/neutrons penetrating through the source transportation channel is apparent. It is visible, that transportation channel plugging has no (for photons) and very low (for neutrons) influence on flux densities in the reference point. Rather unexpected are relatively high calculated differences between model with source symmetrical approximation and model with source transportation system full description evident for photons (Fig. 10) as well as photon field asymmetry for lower elevation angles caused by the real source design and presence of the source transportation system. Rather surprising is also calculated decrease of the neutron flux densities for detector on the transport channel axis (see Fig. 11).

3.3 Calculated Spectral Distributions

Spectral distributions for all presented above (see par. 3.2) values were calculated. Comparison of photons energy distributions for configuration with floor was done. Arrangements for simplified source description and reference point, full source/rabbit holder description

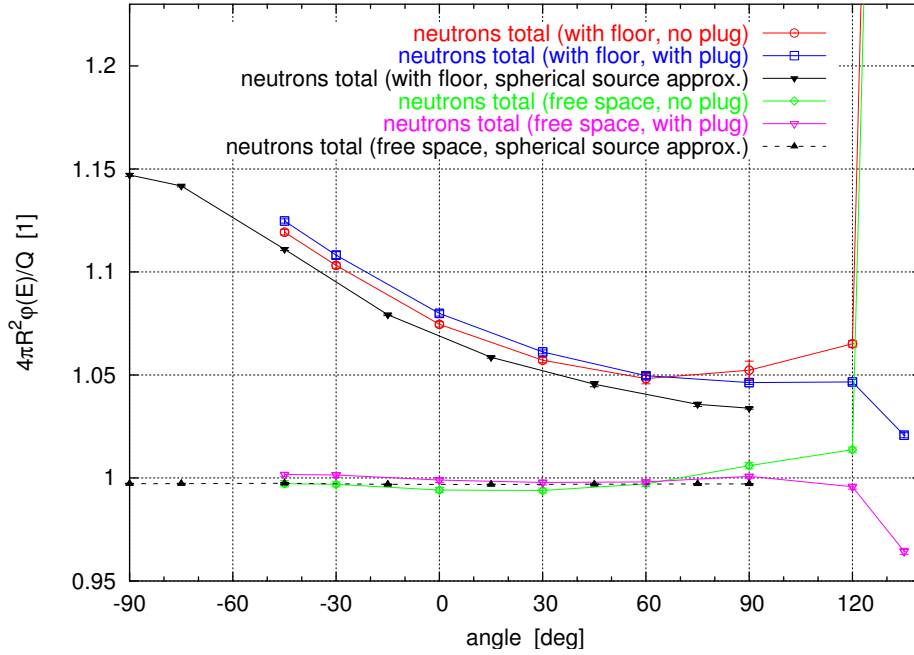


Figure 11: FE50R100 set-up, calculated dependence of the normalized neutron flux density on angle of elevation (in the plane of rabbit holder, real detector position=0 deg, rabbit holder axis=135 deg, $\pm 3\sigma$ error bars)

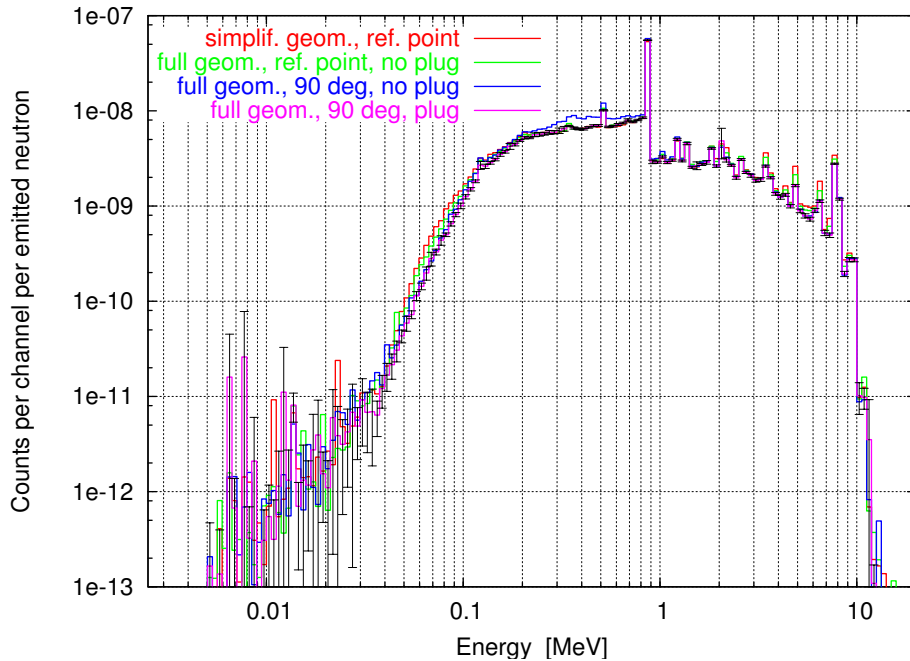


Figure 12: FE50R100 set-up, comparison of calculated photon spectra for different experimental arrangements and point detector positions ($\pm 2\sigma$ error bars added to full geom., 90 deg, with plug case as example)

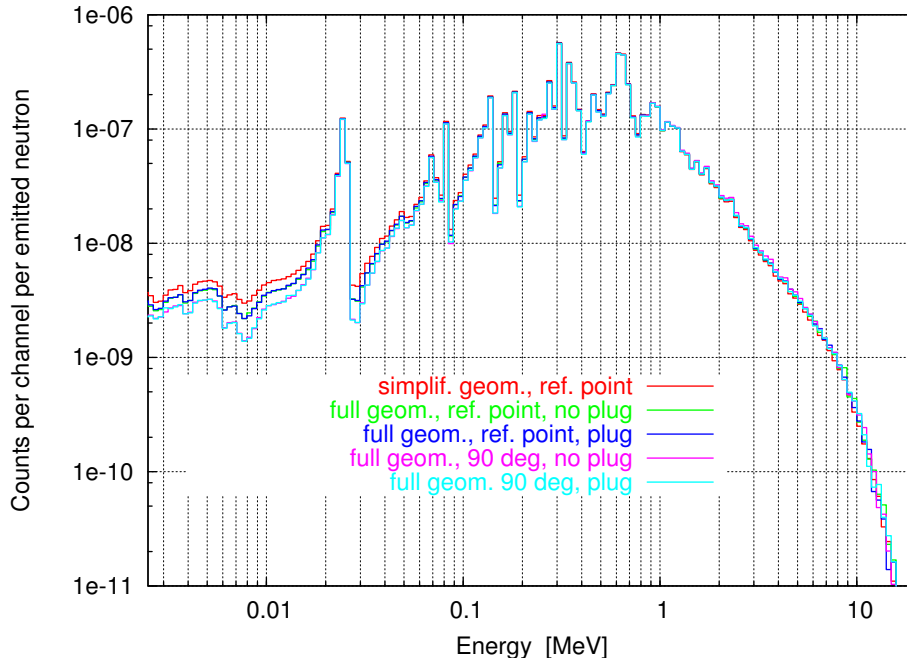


Figure 13: FE50R100 set-up, comparison of calculated photon spectra for different experimental arrangements and point detector positions (errors in confidence level $\pm 2\sigma$ are less than 2%)

without plug and reference point, full source/rabbit holder description without plug and elevation angle 90 deg and full source/rabbit holder description with plug and elevation angle 90 deg were taken into account for photons and spectra presented in the Fig. 12. Spectra of neutrons for the same arrangements and additionally for full source/rabbit holder description with plug and reference point arrangement are shown in the Fig. 13.

4 COMPARISON OF CALCULATED AND EXPERIMENTAL DATA

Comparison of calculated (for FE50R100 arrangement with floor of experimental hall) and experimental data for reference point and neutron and photon flux densities is in Table III. Values calculated for full energy spectra, integrals for energy intervals corresponding to the measurement energy ranges and experimental values are presented. The net effect was determined as difference between results for arrangement without shielding cone and arrangement with corresponding shielding cone (see shielding cone for photons and neutrons respectively). Row for “Calculated net effect” represents calculated contribution from source/sphere (see Tab. I, II) and “Difference” represent studied “secondary effects” – see par. 2. Table shows, that influence of these effects is very low (on the computational error level and significantly lower than typical error of experimental results). On the other hand (see Tab. II) measurements of the photon component for the arrangement with shielding cone Fe+PE(B) for neutrons will be underestimated by about 13% (particularly due to secondary photons from neutron interactions in the polyethylene part of shielding cone). It can be important in the process

of calibration detection systems sensitive to the both reference field components. The similar underestimation for neutrons using arrangement with Pb shielding cone for photons will be only about 3% (see also Tab. II).

Table III: Comparison of calculated and experimental data for FE50R100 arrangement with floor of experimental hall

	neutrons					
	calc. (< 22 MeV)		calc. (0.1-12 MeV)		exper. (0.1-12 MeV)	
	$4\pi R^2\phi(E)/Q$	err ($\pm 1\sigma$)	$4\pi R^2\phi(E)/Q$	err ($\pm 1\sigma$)	$4\pi R^2\phi(E)/Q$	err ($\pm 2\sigma$)
	[1]	[%]	[1]	[%]	[1]	[%]
	Effect+Backgr.	1.068	< 1	0.936	< 1	0.920
Background	0.091	< 1	0.047	< 1	0.095	4.0
Net Effect	0.977	< 1	0.889	< 1	0.825	3.3
Calc. Net Effect	0.970	< 1	0.881	< 1		
Difference	0.007		0.008			
	photons					
	calc. (0.005-22 MeV)		calc. (0.6-10 MeV)		exper. (0.6-10 MeV)	
	$4\pi R^2\phi(E)/Q$	err ($\pm 1\sigma$)	$4\pi R^2\phi(E)/Q$	err ($\pm 1\sigma$)	$4\pi R^2\phi(E)/Q$	err ($\pm 2\sigma$)
	[1]	[%]	[1]	[%]	[1]	[%]
	Effect+Backgr.	0.0440	< 1	0.0243	< 1	0.052
Background	0.0047	< 1	0.0018	< 1	0.027	7.0
Net Effect	0.0392	< 1	0.0225	< 1	0.025	17.0
Calc. Net Effect	0.0391	< 1	0.0225	< 1		
Difference	0.0001		~0			

5 CONCLUSIONS

The Monte Carlo technique enables to study effects and processes that can't be differentiated or separated and evaluated experimentally. Using this advantage, the individual components of the neutron and gamma reference mixed field were studied for different arrangements of shadow shield technique measurements. Calculations show that studied effects are very low and practically negligible in comparison with experimental error. Exception is underestimation of photon component measuring in arrangement with neutron shielding cone. It can be significant for calibrations of detection systems sensitive to the both field components (e.g. some TLD systems). Studies of field inhomogeneity due to source asymmetry, source transportation system and transportation channel show differences between simplified and real model. It was calculated, that transportation system plugging has very low or negligible effect on mixed field parameters in the reference point.

6 REFERENCES

1. B. Jansky, P. Otopal, E. Novak, "Data for Calculation of Neutron and Gamma Leakage Spectra from Iron and Water Spheres with Cf-252 Neutron Source in Centre," Report NRI, UJV-11506, INIS : E 4120, E 21.00, pp.2-26 (Řež 2000).

2. B. Janský, E. Novák, Z. Turzík, J. Kyncl, F. Cvachovec, J. Klusoň, L. A. Trykov, V. S. Volkov, P. Čuda, "Comparison of Measured and Calculated Mixed Neutron and Gamma Fields in Iron and Water Benchmark Assemblies Driven by Cf-252 Neutron Source," *Proceedings of 11th International Symposium on Reactor Dosimetry*, Brussels, Belgium, 18-23 August 2002, World Scientific Publishing, pp. 519-527 (2003).
3. B. Janský, E. Novák, Z. Turzík, J. Kyncl, F. Cvachovec, J. Klusoň L. A. Trykov, V. S. Volkov, P. Čuda, "Mixed Neutron and Gamma Spectra Measurements and Calculations in Pure Iron Benchmark Assembly with Cf-252 Neutron Source," *Proceeding of International Conference on Nuclear data for Science and Technology*, ND 2001, Tsukuba, Ibaraki, Japan 2001, in *Journal of Nuclear Science and Technology Supplement 2*, **Volume 2**, pp.1033-1036 (2002).